

# Influence of Ionic Interactions on the Crystallization of Lightly Sulfonated Syndiotactic Polystyrene Ionomers

E. Bruce Orler and Robert B. Moore\*

Department of Polymer Science, University of Southern Mississippi,  
P.O. Box 10076, Hattiesburg, Mississippi 39406-0076

Received March 10, 1994; Revised Manuscript Received May 23, 1994\*

**ABSTRACT:** The effect of ionic interactions on the crystallization behavior of lightly sulfonated syndiotactic polystyrene (SsPS) ionomers has been evaluated for systems containing 0.5 and 2.0 mol % sulfonate groups. In agreement with studies of other semicrystalline ionomers, the rate of SsPS crystallization decreases with increasing sulfonation and neutralization. For the neutralized ionomers containing 2 mol % sulfonation, the size of the alkali metal counterion was found to have a significant effect on the rate of crystallization. SsPS ionomers containing large Cs<sup>+</sup> ions crystallized at about twice the rate of the ionomers neutralized with small K<sup>+</sup> ions. From SALS and SAXS results, isothermally crystallized SsPS ionomers were found to form spherulitic superstructures in the presence of ionic aggregates. These ionic domains were found to have an average intermultiplet spacing which is identical to that of sulfonated *atactic* polystyrene ionomers. In addition, wide-angle X-ray diffraction studies showed that the polymorphic crystal structures of sPS are strongly influenced by the incorporation of small quantities of ionic groups along the polymer backbone. Under isothermal crystallization conditions, the SsPS ionomers were found to preferentially organize into the  $\beta$ -form crystal structure.

## Introduction

Many studies of industrially important ionomers have demonstrated that the desirable chemical and physical properties of these materials are strongly dependent on the size, quantity, and distribution of ionic multiplets and crystalline domains in the polymer.<sup>1</sup> During the development of this complex morphology, it is important to note that each polymer chain is likely to traverse both the ionic and crystalline domains. Consequently, crystallization is expected to be influenced by the extent of ionic interactions, and ionic aggregation is expected to be affected by crystallization. Thus, systematic control over the formation of the crystalline and ionic domains must be achieved to tailor the properties of semicrystalline ionomers for specific applications.

Previous investigations of semicrystalline ionomers have focused primarily on polyethylene-based systems.<sup>2-9</sup> These studies have demonstrated that the degree of crystallinity decreases with an increase in the ionizable comonomer content (i.e., an increase in the quantity of noncrystallizable monomer units) and with an increase in the degree of ionization (i.e., the fraction of acidic monomer units which have been neutralized).<sup>2,3</sup> Furthermore, investigations of these ionomers have shown that the crystalline morphology is qualitatively similar to that of the homopolymer;<sup>2,4</sup> however, the rate of crystallization decreases with an increase in the quantity of ionic groups.<sup>5</sup> While the effect of ionic content on the degree of ionomer crystallinity may be partially accounted for by the incorporation of noncrystallizable monomer units, the current understanding of the fundamental effects of ionic aggregation on ionomer crystallization remains limited.

To address the lack of critical information regarding the complex morphology of semicrystalline ionomers, we have begun an investigation aimed at understanding the link between ionic aggregation and crystallization. Although the structure-property relationships of the industrially important ethylene-based ionomer systems have been extensively studied,<sup>2-7</sup> undesirable microstructural

characteristics (e.g., variation in molecular weight between copolymers of different ion content and random, poly-disperse alkyl chain branching along the backbone) of the resulting copolymers prevents these materials from being acceptable model systems for morphological studies.

Since a wealth of experimental and theoretical information regarding ionic aggregation exists for sulfonated *atactic* polystyrene (SaPS) ionomers,<sup>10-18</sup> the optimum choice of a semicrystalline ionomer for fundamental investigations is lightly sulfonated stereoregular polystyrene (e.g., sulfonated syndiotactic polystyrene (SsPS)). By comparing the effects of ionic aggregation on the structure-property relationships of SsPS to that of SaPS ionomers, the role of crystalline domains in governing the properties of semicrystalline ionomers may be obtained. Of specific interest in this investigation, syndiotactic polystyrene (sPS) crystallizes very rapidly and exhibits several polymorphic crystal structures.<sup>19-25</sup> In this study, the influence of ionic interactions on the crystallization kinetics and formation of polymorphic crystalline domains in lightly sulfonated syndiotactic polystyrene ionomers is examined.

## Experimental Section

**Materials.** Syndiotactic polystyrene (with >99% syndiotactic purity) was obtained from the Dow Chemical Co. and had a weight-average molecular weight of 609 000. All other chemicals and solvents were obtained from Aldrich and used without further purification.

The syndiotactic polystyrene was sulfonated using acetyl sulfate in 1,2,4-trichlorobenzene as previously described.<sup>26,27</sup> The degree of sulfonation was determined by nonaqueous titration, using a methanolic KOH titrant, to the phenolphthalein end point. The titrant was calibrated using a benzoic acid standard dissolved in trichlorobenzene. The sample titrations were conducted at 70 °C in solutions containing 0.5 g of SsPS in 100 mL of 95:5 (v/v) trichlorobenzene-ethanol solvent. Once the degree of sulfonation was determined, the SsPS samples were neutralized by dissolving 0.5 g of SsPS in 20 mL of trichlorobenzene and adding a stoichiometric amount of methanolic KOH or CsOH. After neutralization, a majority of the solvent was removed by freeze-drying. The samples were washed with methanol and then completely dried in a vacuum oven at 70 °C for 48 h.

\* Author to whom all correspondence should be addressed.

© Abstract published in *Advance ACS Abstracts*, July 1, 1994.

**Characterization Methods.** The thermal properties and crystallization kinetics of the sPS and SsPS ionomers were compared using Perkin-Elmer DSC 7 differential scanning calorimeter with a nitrogen purge. The glass transition temperatures,  $T_g$ 's, were determined as the midpoint of the step change in the heat flow. The melting,  $T_m$ , and crystallization,  $T_c$ , temperatures were selected as the peak maximum or minimum in endothermic or exothermic transitions, respectively.

To eliminate possible differences in thermal history, the crystallization kinetics were obtained for samples which were annealed at 330 °C for 3 min. The samples were then cooled at -200 °C/min to the crystallization temperature, and the crystallization exotherm was monitored with time. The crystallization data were analyzed using the Avrami equation,<sup>28</sup>

$$\log[-\log(1 - X_t)] = \frac{1}{2.3} \log K + n \log t \quad (1)$$

where  $X_t$  is the weight fraction of material crystallized at time  $t$ ,  $K$  is the kinetic growth rate constant, and  $n$  is the Avrami exponent.

Equilibrium melting temperatures were evaluated using a Mettler FP82HT hot stage mounted on a Nikon Optiphot2 polarizing optical microscope. The samples were heated in a nitrogen atmosphere to 330 °C, held for 3 min, and then cooled at ca. -20 °C/min to the crystallization temperature. After the samples had crystallized, they were heated from 250 °C at 1 °C/min. The optical melting point was chosen as the temperature at which all birefringence had disappeared. The equilibrium melting temperature,  $T_m^0$ , was determined by plotting the optical melting point versus crystallization temperature for each sample; the point of intersection between the theoretical line defined by  $T_m = T_c$  and the extrapolated experimental data yields the equilibrium melting temperature.

Small-angle light scattering (SALS) patterns are obtained using a laser light scattering device similar to that described by Stein and Rhodes.<sup>29</sup> The incident light was obtained from a 3 mW He-Ne laser (Oriol Corp., Model 6697), and the scattered  $H_v$  patterns were recorded on Polaroid type 55 film. The spherulitic radii,  $R$ , were calculated from the  $H_v$  patterns using the relationship

$$R = \frac{1.025\lambda_0/n}{\pi \sin(\theta_m'/2)} \quad (2)$$

where  $\lambda_0$  is the wavelength of light in air,  $n$  is the sample refractive index, and  $\theta_m$  is the corrected scattering angle at maximum intensity. The scattering angle is corrected for refraction at the sample surface by the relationship  $n = \sin \theta_m / \sin \theta_m'$ , where  $\theta_m$  is the experimentally observed scattering angle at maximum intensity.<sup>30</sup>

Wide-angle X-ray diffraction (WAXD) data for isothermally crystallized sPS and SsPS ionomers were obtained using a Siemens XPD-700P polymer diffraction system equipped with a 2 kW, sealed-tube, Cu K $\alpha$  photon source and a two-dimensional, position-sensitive area detector. The samples (prepared in the DSC) were first heated at 330 °C for 3 min to eliminate possible differences in thermal history. The samples were rapidly cooled at -200 °C/min to the isothermal crystallization temperature and then annealed for 1 h. Finally, these samples were quenched to room temperature, removed from the DSC pans, and mounted in the WAXD sample holder. All data were collected in the transmission mode with a sample-to-detector distance of 10 cm. After background subtraction, the diffractograms were obtained by radially integrating the two-dimensional diffraction patterns using the GADDS software package.

With a method developed by Guerra and co-workers,<sup>24</sup> quantitative analysis of the polymorphic crystal structures was performed by deconvoluting and measuring the integrated peak areas of the  $\alpha$  and  $\beta$  reflections at 11.6 and 12.2° 2 $\theta$ , respectively. The percent  $\alpha$  crystal form,  $P_\alpha$ , was then calculated using the relationship

$$P_\alpha = \frac{1.8A_{11.6}/A_{12.2}}{1 + 1.8A_{11.6}/A_{12.2}} \times 100 \quad (3)$$

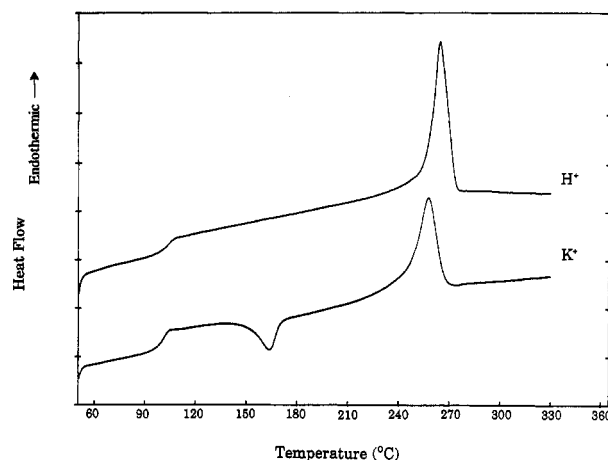


**Figure 1.** Effect of neutralization on the DSC scans of melt-quenched syndiotactic polystyrene containing 0.5 mol % sulfonation.

where  $A_{11.6}$  and  $A_{12.2}$  are the areas under peaks centered at 2 $\theta$  of 11.6 and 12.2°, respectively.

Small-angle X-ray scattering (SAXS) was also performed using the Siemens XPD-700P polymer diffraction system. All data were collected in the transmission mode with a sample-to-detector distance of 49 cm. To avoid excess air scatter, the scattering path from the sample to the detector was sealed and purged with helium gas. The SAXS data are plotted as the relative intensity versus  $q$ , where  $q = (4\pi/\lambda) \sin \theta$ ,  $\theta$  is half the scattering angle and  $\lambda$  is the X-ray wavelength ( $\lambda = 0.154$  nm).

## Results and Discussion

**Effect of Ionic Interactions on the Thermal Properties of SsPS.** Figure 1 shows DSC scans of the 0.5 mol % acid-form and potassium-neutralized SsPS ionomers which had been quenched from the melt. Prior to collecting the heating scan data, the samples were first heated to 330 °C and then rapidly cooled at a rate of -200 °C/min to the start temperature of 50 °C. While the DSC scan of the H<sup>+</sup>-form sample containing 0.5 mol % acid groups is similar to that observed for pure syndiotactic polystyrene,<sup>26</sup> a notable change in the thermal properties is observed for the K<sup>+</sup>-neutralized sample. The absence of a crystallization exotherm in the thermogram of the H<sup>+</sup>-form sample indicates that the polymer crystallizes completely during the quenching cycle. For the K<sup>+</sup>-neutralized sample, however, the appearance of a crystallization exotherm, at about 165 °C, indicates that the time period during the quench was insufficient to allow for complete crystallization of the neutralized ionomer. This behavior suggests that the rate of crystallization is retarded for the K<sup>+</sup>-neutralized ionomer relative to the unneutralized SsPS.

Figure 2 shows the DSC scans of the acid-form and K<sup>+</sup>-neutralized SsPS samples containing 2 mol % sulfonation. Curves A and B are the reheating scans for the acid and K<sup>+</sup>-neutralized ionomers which had been quenched from the melt, while curve C is the thermogram of isothermally crystallized K<sup>+</sup>-form SsPS. The thermal behavior of the H<sup>+</sup>-form sample is qualitatively similar to that of the K<sup>+</sup>-neutralized 0.5 mol % sample shown in Figure 1; the appearance of a crystallization exotherm again indicates that the time period during the quench was insufficient to allow for complete crystallization. Thus, in agreement with studies of other semicrystalline ionomers,<sup>2,5</sup> a comparison of the 2.0 mol % H<sup>+</sup>-form SsPS thermogram (Figure 2A) to the data in Figure 1 suggests that increasing the level of sulfonation in SsPS also retards the rate of crystallization.

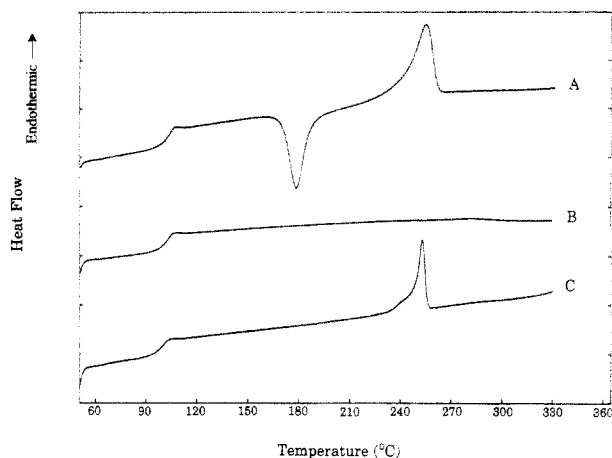


**Figure 2.** Effect of neutralization and thermal history on 2.0 mol % sulfonated syndiotactic polystyrene ionomers: (A) melt-quenched SsPS-2.0H<sup>+</sup>; (B) melt-quenched SsPS-2.0K<sup>+</sup>; (C) SsPS-2.0K<sup>+</sup> annealed at 225 °C for 1 h.

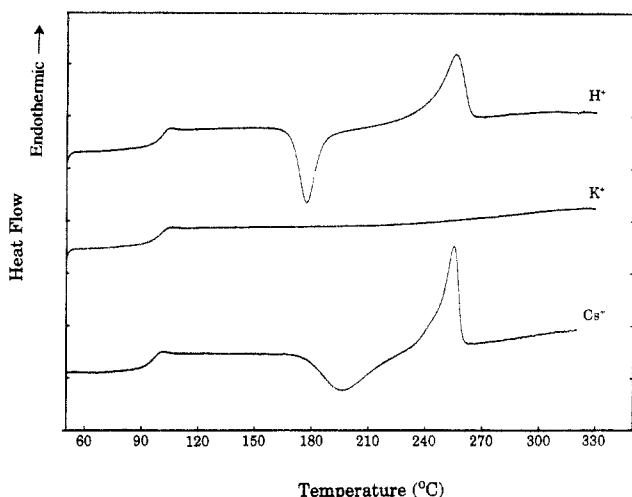


**Figure 3.** Effect of counterion type on the thermal properties of melt-quenched SsPS ionomers containing 2 mol % sulfonation.

For the K<sup>+</sup>-neutralized 2.0 mol % SsPS sample (Figure 2, curve B), the lack of a crystallization exotherm or a melting endotherm indicates that the material does not crystallize during the heating scan or possess significant crystallinity. However, after the 2 mol % K<sup>+</sup>-form SsPS had been isothermally crystallized (from the melt) at 225 °C for 1 h, a significant degree of crystallinity was reintroduced, and a DSC scan (curve C) of this annealed sample displayed a sharp melting endotherm.

The crystallization behavior of the K<sup>+</sup>-form ionomers may be attributed to the retardation effects of ionic aggregation on the crystallization kinetics. As ionic aggregates are formed, strong Coulombic interactions between the ion pairs create electrostatic cross-links which restrict the mobility of the polymer chains. This restricted mobility thus suppresses crystallization during the quench or subsequent heating scans. Under isothermal crystallization conditions, however, this small quantity of ionic groups does not prevent crystallization but simply retards the rate of crystallization.

Figure 3 shows the effect of changing the counterion on the thermal behavior of melt-quenched SsPS ionomers containing 2 mol % sulfonation. In contrast to the lack of crystallinity observed for the melt-quenched, K<sup>+</sup>-neutralized sample, the Cs<sup>+</sup>-neutralized ionomer crystallizes to a significant degree within the time frame of the DSC heating scan. Furthermore, the final degree of crystallinity for the Cs<sup>+</sup>-neutralized sample is quite similar

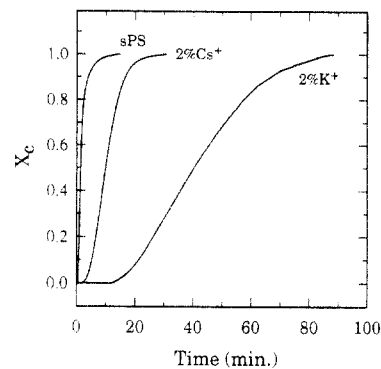


**Figure 4.** Fractional crystallization versus time profiles for sPS and SsPS-2.0 ionomers isothermally crystallized at a supercooling of 40 °C.

to that of the H<sup>+</sup>-form SsPS. It is important to note, however, that the crystallization exotherm for the melt-quenched, Cs<sup>+</sup>-neutralized sample is broader and ca. 15 °C higher than that of the H<sup>+</sup>-form SsPS. This crystallization behavior may be explained by comparing the strengths of interactions between the sulfonated styrene units.

Previous investigations of sulfonated polystyrene (SaPS) ionomers have shown that electrostatic attractive forces between the ion pairs in a multiplet containing Cs<sup>+</sup> sulfonate groups are weaker than those in samples neutralized with smaller alkali metal ions.<sup>31-34</sup> Since strong ionic interactions within multiplets tend to inhibit ion hopping<sup>34,35</sup> (i.e., the dynamic behavior of ion pairs transferring from multiplet to multiplet in an attempt to satisfy the local balance between electrostatic and elastic forces), it is expected that chain mobility, which is required for significant crystallization, would be less in the K<sup>+</sup> ionomer relative to the Cs<sup>+</sup> ionomer.<sup>34</sup> Furthermore, the amount of thermal energy required to increase ion hopping to a rate which provides sufficient chain mobility for crystallization should increase with the strength of the ionic interactions. Thus, based on this chain mobility argument, the sluggish chains of the K<sup>+</sup>-neutralized SsPS were unable to crystallize during the heating scan, while the more mobile chains of the Cs<sup>+</sup>-neutralized SsPS had sufficient time to organize.

In comparing the thermal behavior of the Cs<sup>+</sup>-neutralized SsPS to that of the H<sup>+</sup>-form sample (Figure 3), it is important to note that, at temperatures above the  $T_g$ , the strength of hydrogen-bonding interactions between SO<sub>3</sub>H groups is weaker than the strong ionic interactions between neutralized sulfonate groups.<sup>16</sup> Moreover, the weak interactions between sulfonic acid groups are much less effective in reducing the chain-segment mobility relative to that of the strong electrostatic cross-links in the Cs<sup>+</sup>-neutralized SsPS. Subsequently, the H<sup>+</sup>-form sample crystallizes at a significantly lower temperature and over a narrower temperature range as compared to the Cs<sup>+</sup>-neutralized sample.

To better understand the effect of ionic aggregation on the crystallization of SsPS, isothermal crystallization kinetics studies were performed. Figure 4 compares the fractional crystallization,  $X_c$ , versus time profile of sPS to those of K<sup>+</sup>- and Cs<sup>+</sup>-neutralized SsPS ionomers containing 2 mol % sulfonate groups. Note that these crystallization profiles were obtained at a similar supercooling ( $\Delta T = T_m^\circ - T_c$ ) of ca. 40 °C. While the ionomers crystallize over a larger period of time relative to the sPS sample, it is clear that the rate of crystallization for the Cs<sup>+</sup>-form SsPS sample is much faster than that for the K<sup>+</sup>-form SsPS.

**Table 1. Summary of Isothermal Crystallization Kinetics Data for sPS, SsPS Ionomers, and iPS**

sample	$T_c$ (°C)	$\Delta T$ (°C)	$t_{1/2}$ (min)	$n$	$K$ (min <sup>-1</sup> )
pure sPS	235	40	1.3	2.3	0.34
sPS-2.0Cs <sup>+</sup>	223	41	19	2.2	$9.7 \times 10^{-4}$
sPS-2.0K <sup>+</sup>	223	39	40	2.5	$7.8 \times 10^{-5}$
pure iPS <sup>a</sup>	197	~40	270	2.9	$3.5 \times 10^{-8}$
sPS-2.0Cs <sup>+</sup>	210	54	10	2.6	$2.0 \times 10^{-3}$
sPS-2.0K <sup>+</sup>	210	52	23	2.4	$3.3 \times 10^{-4}$

<sup>a</sup> Obtained from ref 36.

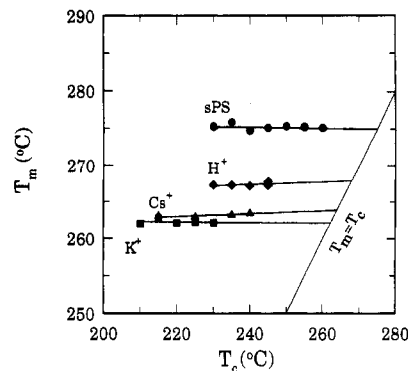
Table 1 compares the bulk crystallization kinetics of the SsPS ionomers to that of pure sPS and isotactic polystyrene (iPS) isothermally crystallized at comparable supercoolings ( $\Delta T \approx 40$  °C). The iPS data are shown to demonstrate that the effect of sulfonation on the crystallization kinetics of a sPS are relatively minor in comparison to a complete change in tacticity. For pure sPS, the crystallization half-time,  $t_{1/2}$ , and the Avrami coefficient,  $n$ , agree with the results obtained by Cimmino and co-workers.<sup>19</sup> The noninteger Avrami coefficients, between 2 and 3, for the sPS and SsPS ionomers suggest that a mixture of nucleation and growth mechanisms are occurring; this behavior is consistent with the polymorphic crystallization of syndiotactic polystyrene.<sup>24,25</sup> Although ionic interactions are clearly important in influencing the overall rate of crystallization, it is interesting to note that the values of the Avrami coefficients for the sPS and SsPS samples are quite comparable. Therefore, the Avrami analysis of these samples suggests that sulfonation and neutralization does not significantly alter the observed crystallization mechanism of syndiotactic polystyrene.

For the ionomers containing as little as 2 mol % ionic species, the relative values of the  $t_{1/2}$  and crystallization rate constant,  $K$ , indicate a significant decrease in the rate of crystallization in comparison to sPS. While the rate of crystallization for the ionomers is expected to be suppressed by the presence of noncrystallizable comonomer units<sup>37</sup> and possible interchain interactions due to ionic aggregation,<sup>5</sup> it is important to note that the Cs<sup>+</sup>-neutralized sample crystallizes at a rate about twice that of the K<sup>+</sup>-neutralized sample. This behavior is also observed when the SsPS ionomers are crystallized at higher supercoolings (i.e.,  $T_c$  decreased from 223 to 210 °C). In agreement with the discussion above, the rate of ion hopping decreases with increasing strength of the electrostatic cross-links. Moreover, since chain-segment mobility is directly dependent on the rate of ion hopping,<sup>34</sup> it is reasonable to expect that the transport of chain segments across the melt/crystal interface will become slower with an increase in the strength of electrostatic interactions. Thus, strong electrostatic cross-links in the K<sup>+</sup>-SsPS, as compared to those in Cs<sup>+</sup>-SsPS, diminish the rate in which the chain segments organize into crystalline domains.

Figure 5 shows the effect of incorporating noncrystallizable, sulfonated styrene units into the polymer backbone on the equilibrium melting temperature,  $T_m^\circ$ , of syndiotactic polystyrene. Flory proposed that the melting point depression for a random, crystallizable copolymer incorporating noncrystallizable monomer units can be calculated following the relationship<sup>38</sup>

$$\frac{1}{T_m} - \frac{1}{T_m^\circ} = -\frac{R}{\Delta H_u} \ln n \quad (4)$$

where  $T_m^\circ$  is the equilibrium melting point of the analogous homopolymer (i.e., sPS),  $T_m$  is the melting point of the copolymer (i.e., SsPS),  $R$  is the gas constant,  $\Delta H_u$  is the

**Figure 5.**  $T_m$  versus  $T_c$  plots for sPS and SsPS-2.0 ionomers.

heat of fusion per mole of crystallizable units, and  $n$  is the mole fraction of crystallizable units. Pasztor and co-workers determined the  $\Delta H_u$  for pure sPS to be 5.58 kJ/mol.<sup>39</sup> In agreement with recent investigations,<sup>19,40-42</sup> unsulfonated sPS yields an equilibrium melting point in the range of 275 °C.

Using Flory's copolymer analysis,<sup>38</sup> the melting point depression for a sPS copolymer containing 2 mol % noncrystallizable monomer units is predicted to be 9 deg. For the H<sup>+</sup>-form SsPS containing 2.0 mol % sulfonated styrene units, the experimentally observed melting point depression is 7 deg. Since the theoretically predicted melting point depression is dependent on the choice of an experimentally determined  $\Delta H_u$ , the calculated and observed melting point depressions are in excellent agreement. Therefore, in agreement with Hsu and co-workers,<sup>43</sup> these data indicate that the bulky sulfonic acid units are not incorporated into the sPS crystalline lattice and reside only in the amorphous phase.

Once the H<sup>+</sup>-form SsPS is neutralized to the K<sup>+</sup> and Cs<sup>+</sup> forms, the  $T_m^\circ$  is depressed to 262 and 264 °C, respectively. These  $T_m^\circ$  values correspond to enhanced melting point depressions of 13 and 11 deg for the neutralized ionomers. This behavior, which is similar to that observed with ethylene-based ionomers,<sup>3</sup> demonstrates that the ionic groups inhibit crystal growth along the polymer chain direction (i.e., obstruct lamellar thickening) to an extent greater than that expected from the simple noncrystallizable-comonomer exclusion effect.<sup>38</sup> Although neutralization has been shown to affect the melting behavior of other semicrystalline ionomers,<sup>2,3,5,7,9</sup> no precise explanation for the influence of ionic interactions on the melting point depression has been proposed.

Since each of the polymer chains in the SsPS ionomers is likely to be involved in the formation of both crystalline and ionic domains, a possible explanation for the observed melting behavior of the neutralized SsPS ionomers may be offered by evaluating the state of ionic aggregation. Figure 6 shows the small-angle X-ray scattering (SAXS) profiles for SsPS containing 2 mol % cesium sulfonate groups (curve A) and pure sPS (curve B). In comparison to the nonionic sPS, the SAXS data for the SsPS ionomer show a broad "ionic" peak which is characteristic of many ionic materials containing multiplets.<sup>11,13,14,44-47</sup> It is important to note that the position of the peak maximum ( $q_{\max} = 1.5 \text{ nm}^{-1}$ ) corresponds to a Bragg spacing of ca. 4.2 nm; this dimension is identical to that observed in sulfonated atactic polystyrene ionomers.<sup>11</sup> Thus, these data indicate that the strong Coulombic interactions between the ionic groups in SsPS yield ionic aggregates which are very similar to those found in the noncrystalline, atactic polystyrene ionomers. Moreover, with respect to the isothermal crystallization data (Table 1), these ionic

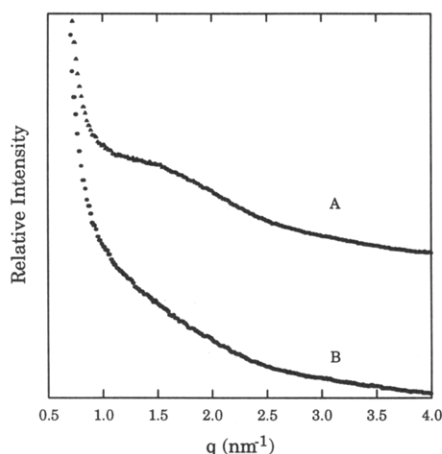


**Figure 6.** Small-angle X-ray scattering profiles of (A) SsPS-2.0Cs<sup>+</sup> and (B) pure sPS. All SAXS samples were crystallized at 210 °C for 1 h.

aggregates form in the presence of a rapidly crystallizing system.

According to a recently proposed theory describing the morphology and properties of random ionomers,<sup>48</sup> the conformational freedom of polymer chain segments attached to the ionized units becomes restricted as the ion pairs aggregate into multiplets. Consequently, it may be difficult to pack the polymer chains, within these regions of restricted mobility, into the conformationally ordered crystalline state observed in syndiotactic polystyrene. Thus, the average length of crystallizable chain segments between ionic monomer units may be effectively reduced by the restricted mobility effects of ionic aggregation. This reduction in the average length of chain segments that can be incorporated into the crystalline lamella inhibits thickening which consequently reduces the  $T_m$  (Figure 5).

In agreement with the effects of multifunctional electrostatic cross-links on the thermal behavior of SsPS, it is interesting to note that Mandelkern et al.<sup>49</sup> observed greater melting point depression for radiation-cross-linked polyethylene relative to that predicted for a random copolymer. This behavior was rationalized by assuming that the number of units that are restricted from participating in the development of crystallinity is appreciably greater than the number of units that are actually intermolecularly cross-linked. Furthermore, Gent<sup>50</sup> found that chemical cross-links in natural rubber retarded the rate of crystallization to an extent greater than that predicted from an elementary banned volume mechanism. This behavior was then attributed in part to a reduction in the mobility of chain segments in the vicinity of cross-links. While these comparisons suggest that the influence of electrostatic cross-links on crystallization is analogous to that of covalent cross-links, it is important to note that ionic multiplets are dynamic in nature<sup>34</sup> and the counterion type plays a prominent role in governing the strength of the electrostatic cross-link.

**Effect of Ionic Interactions on the Crystalline Morphology of SsPS.** Figure 7 compares the  $H_v$  (i.e., horizontal polarizer with vertical analyzer) small-angle light scattering (SALS) patterns of pure sPS to that of the 2 mol % SsPS ionomers neutralized with Cs<sup>+</sup> and K<sup>+</sup> ions. Note that all samples were isothermally crystallized at a supercooling of 40 °C for ca. 1 h (or until the sample was volume-filled with spherulites as observed by polarized optical microscopy). Since each sample shows the typical four-lobe scattering pattern characteristic of a spherulitic superstructure, these data demonstrate that incorporation of up to 2 mol % of covalently-attached ionic groups onto

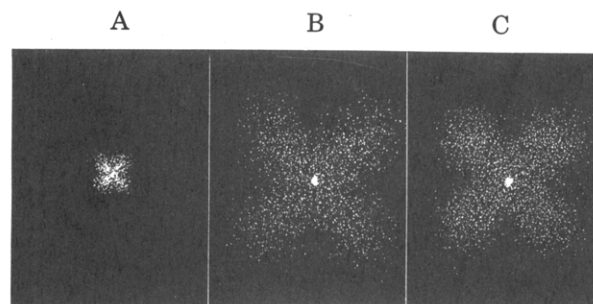


**Figure 7.**  $H_v$  small-angle light scattering patterns of (A) sPS, (B) SsPS-2.0K<sup>+</sup>, and (C) SsPS-2.0Cs<sup>+</sup>. All SALS samples were crystallized at 210 °C for 1 h.

the sPS chain does not disrupt the spherulitic organization of the crystallites in SsPS ionomers.

Based on the constant sample-to-film distance used to obtain each of the SALS patterns in Figure 7, the average radius of the spherulites was calculated according to eq 2 (see Experimental Section). The relatively small SALS pattern for the pure sPS sample yields an average spherulite radius of 10  $\mu\text{m}$ . In contrast, the average spherulitic radii for the 2 mol % K<sup>+</sup>- and Cs<sup>+</sup>-form SsPS ionomers were found to be 2.6 and 4.4  $\mu\text{m}$ , respectively. Since the SALS samples were crystallized until volume-filled, the smaller spherulites in the SsPS ionomers relative to those of the pure sPS may be attributed to an increased nucleation density and a significantly retarded growth rate. This increased nucleation is likely to be associated with the presence of ionic aggregates which influence the mobility of polymer chains in the melt. However, due to the apparent mixture of nucleation and growth mechanisms, as suggested from the noninteger Avrami coefficients (Table 1), further kinetic investigations of spherulitic growth in SsPS ionomers will be required to understand the effect of ionic aggregation on nucleation.

While the DSC data clearly demonstrate that SsPS ionomers contain significant degrees of crystallinity, further insight into the effects of ionic interactions on the complex morphology of sPS crystalline domains may be obtained using X-ray diffraction methods. Of specific interest, previous WAXD investigations have shown that melt-crystallized sPS exhibits two distinct polymorphic crystalline structures.<sup>24,25</sup> Both of these crystal structures have been found to arise from ordered packing of planar zigzag sPS chains; the  $\alpha$ -form unit cell is composed of a hexagonal array of three chain clusters, and the  $\beta$ -form unit cell is composed of an orthorhombic arrangement of sPS chains.<sup>25</sup> De Rosa and co-workers<sup>25</sup> showed that the thermodynamically favored  $\beta$  crystal structure<sup>51</sup> may be obtained when the melt is slow cooled, whereas the kinetically favored  $\alpha$  crystal structure is produced when the melt is rapidly cooled. Furthermore, intermediate cooling rates were found to produce a mixture of the two crystal forms.

Figure 8 compares the WAXD profiles of pure sPS isothermally crystallized at 250 and 210 °C to that of the 0.5 and 2.0 mol % K<sup>+</sup>-form SsPS ionomers isothermally crystallized at 210 °C. The diffractogram of sPS crystallized at 250 °C (curve A) exhibits reflections indicative of a predominantly  $\beta$  crystal form ( $P_\alpha = 10\%$ ), whereas the crystal structure of the sPS crystallized at 210 °C (curve B) yields a predominant  $\alpha$ -form ( $P_\alpha = 73\%$ ). In comparison to the pure sPS materials, the diffraction patterns of the K<sup>+</sup>-neutralized ionomers, isothermally crystallized at 210 °C (curves C and D), indicate a mixture of the two crystal structures. The percent  $\alpha$  crystal form for the 0.5 and 2.0 mol % neutralized ionomers are approximately 52

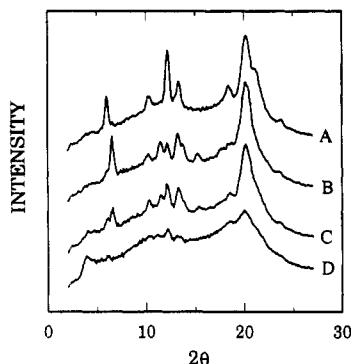


**Figure 8.** Wide-angle X-ray diffractograms of isothermally crystallized sPS and K<sup>+</sup>-form SsPS ionomers: (A) sPS crystallized at 250 °C for 1 h; (B) sPS crystallized at 210 °C for 1 h; (C) SsPS-0.5K<sup>+</sup> crystallized at 210 °C for 1 h; (D) SsPS-2.0K<sup>+</sup> crystallized at 210 °C for 1 h.

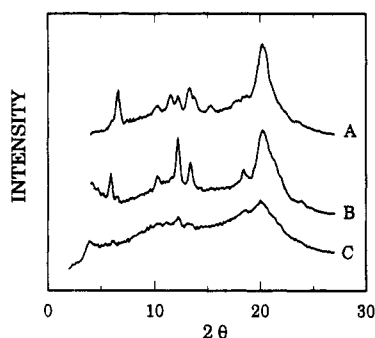


**Figure 9.** Effect of counterion type on WAXD patterns of sPS and 2 mol % SsPS ionomers: (A) sPS; (B) SsPS-2.0Cs<sup>+</sup>; (C) SsPS-2.0K<sup>+</sup>. All samples were isothermally crystallized at 210 °C for 1 h.

and 28%, respectively. Thus, at these crystallization temperatures, the WAXD data indicate that incorporation of small quantities of ionic groups onto sPS favors the formation of the  $\beta$ -form crystal structure.

In addition to revealing the crystal-form compositions, the WAXD profiles in Figure 8 also show that the intensity of the crystalline diffraction peaks decreases by increasing the quantity of ionic groups from 0.5 to 2.0 mol % (curves C and D, respectively). In agreement with the DSC studies of crystallization kinetics (above), the maximum degree of crystallinity obtained for the 2 mol % K<sup>+</sup>-form SsPS ionomer was 15% as compared to ca. 40% for pure sPS. Since the maximum degree of crystallinity was obtained for samples which were isothermally crystallized until  $X_c = 1.0$  (e.g., see Figure 4), the observed decrease in the degree of crystallinity with increasing sulfonation may be attributed to a decrease in the quantity of chain segments of sufficient length to crystallize. However, in light of the data in Figure 5, which show a significant effect of ionic interactions on the formation of crystalline domains in SsPS, an argument based on treating the ionized groups only as noncrystallizable, *noninteracting*, monomer units is clearly an oversimplification.

The profound effect of ionic interactions on SsPS crystallization is further demonstrated by contrasting the crystallization of the K<sup>+</sup> and Cs<sup>+</sup> ionomers. Figure 9 compares the diffractogram of pure sPS, isothermally crystallized at 210 °C, with that of the 2 mol % K<sup>+</sup>- and Cs<sup>+</sup>-neutralized SsPS ionomers. In comparison of the polymorphic crystal forms, the 2 mol % Cs<sup>+</sup>-neutralized SsPS sample contains a much higher  $\beta$ -form composition ( $P_\beta = 13\%$ ) than the pure sPS sample crystallized at the same temperature. It is important to note that the polymorphic composition of the Cs<sup>+</sup>-form SsPS ionomer

is quite comparable to that of pure sPS crystallized at a significantly higher temperature (Figure 8, curve A). Therefore, these data suggest that the choice of counterion and crystallization temperature may be used to selectively manipulate the polymorphic crystal structure of SsPS ionomers.

Finally, by comparing curves B and C of Figure 9, it is clear that the rapidly crystallizing Cs<sup>+</sup>-form ionomer reaches a maximum degree of crystallinity which is much greater than that of the K<sup>+</sup>-form SsPS. Surprisingly, DSC results indicate that the maximum degree of crystallinity obtained for the Cs<sup>+</sup>-form SsPS ionomer is approximately the same as that obtained for pure sPS (i.e.,  $W_c \approx 40\%$ ). Although the difference in maximum crystallinity between the Cs<sup>+</sup>- and K<sup>+</sup>-form ionomers follows the expected trend based on relative strengths of the electrostatic interactions, further investigations of SsPS nucleation, spherulitic growth rate, and melt rheology will be required to understand the high degree of crystallinity observed for the Cs<sup>+</sup>-form ionomer with respect to pure sPS.

## Conclusions

To investigate the link between ionic aggregation and crystallization in semicrystalline ionomers, a model system has been prepared by lightly sulfonating syndiotactic polystyrene.<sup>26</sup> From these studies, it is clear that incorporation of small quantities of sulfonate groups onto crystallizable polystyrene chains has a profound effect on the crystallization of syndiotactic polystyrene. In comparison to pure sPS, the rate of crystallization in SsPS ionomers decreases as the level of sulfonation is increased from 0.5 to 2.0 mol %. The rate of crystallization decreases further as the acid-form samples are neutralized to the K<sup>+</sup> form. For the acid-form SsPS materials, the reduced rate of crystallization is primarily attributed to the incorporation of noncrystallizable groups into the crystalline backbone. However, for neutralized SsPS ionomers, strong ionic interactions tend to restrict the mobility of the crystallizable chain segments and thus reduce the rate of crystallization to a level well below that of H<sup>+</sup>-form SsPS (at the same degree of sulfonation). For SsPS containing 2 mol % sulfonation, neutralization clearly slows the rate of crystallization but does not eliminate the formation of crystalline domains under isothermal crystallization conditions.

With respect to the effects of neutralization on SsPS crystallization, the strength of the ionic interactions, as governed by the choice of neutralizing counterion, is shown to play an important role in the crystallization behavior of SsPS ionomers. At a given crystallization temperature (e.g.,  $T_c = 210$  °C), the strength of the electrostatic cross-links influences the mobility of crystallizable polymer chains by affecting the rate at which ion pairs hop from multiplet to multiplet. When SsPS is neutralized with small K<sup>+</sup> ions, the strength of electrostatic cross-links in the melt is strong compared to that in the same material neutralized with larger Cs<sup>+</sup> counterions.<sup>34</sup> Therefore, the low rate of crystallization observed for the K<sup>+</sup>-neutralized SsPS material is attributed to strong ionic interactions which reduce the chain segment mobility relative to that observed with the Cs<sup>+</sup>-neutralized SsPS.

The use of lightly sulfonated syndiotactic polystyrene as an ideal model system for investigations of semicrystalline ionomers is highlighted by the morphological information obtained in this initial study. While the ionic groups in SsPS aggregate into multiplets which appear to be quite similar to those found in sulfonated, *atactic* polystyrene, the SsPS chain segments between the ionic

groups are still able to crystallize. Moreover, these crystalline domains organize into polymorphic forms and spherulitic superstructures which are comparable to those found in pure sPS. Since the rate and/or degree of crystallization is strongly influenced by the incorporation of ionic groups onto sPS, these studies suggest that the choice of counterion and crystallization conditions may be used to selectively manipulate the composition of the polymorphic crystal structure within SsPS ionomers. Future investigations of these materials will be aimed at understanding the specific manner in which ionic interactions influence the mechanism of polymorphic crystallization within SsPS ionomers.

**Acknowledgment.** The authors gratefully acknowledge the Mississippi NSF EPSCoR Program (Grant No. EHR-9108767) for financial support and the Dow Chemical Co. for supplying the syndiotactic polystyrene.

## References and Notes

- Eisenberg, A.; Bailey, F. E., Eds. *Coulombic Interactions in Macromolecular Systems*; ACS Symposium Series 302; American Chemical Society: Washington, DC, 1986.
- Marx, C. L.; Cooper, S. L. *J. Macromol. Sci., Phys.* **1974**, *B9*, 19.
- Otocka, E. P.; Kwei, T. K. *Macromolecules* **1968**, *1*, 401.
- Wilson, F. C.; Longworth, R.; Vaughan, D. J. *Polym. Prepr. (Am. Chem. Soc., Div. Polym. Chem.)* **1968**, *9*(1), 505.
- Tsujita, Y.; Shibayama, K.; Takizawa, A.; Kinoshita, T. *J. Appl. Polym. Sci.* **1987**, *33*, 1307.
- Otocka, E. P.; Kwei, T. K.; Salovey, R. *Makromol. Chem.* **1969**, *129*, 144.
- Hirasawa, E.; Yamamoto, Y.; Tadano, K.; Yano, S. *J. Appl. Polym. Sci.* **1991**, *42*, 351.
- Phillips, P. J.; Emerson, F. A.; MacKnight, W. J. *Macromolecules* **1970**, *3*, 767.
- Rahrig, D.; MacKnight, W. J. In *Ions in Polymers*; Eisenberg, A., Ed.; Advances in Chemistry Series 187; American Chemical Society: Washington, DC, 1980; Chapter 7.
- Fitzgerald, J. J.; Weiss, R. A. *J. Macromol. Sci., Rev. Macromol. Chem. Phys.* **1988**, *C28*, 99.
- Weiss, R. A.; Lefelar, J. A. *Polymer* **1986**, *27*, 3.
- Register, R. A.; Cooper, S. L. *Macromolecules* **1990**, *23*, 310.
- Yarusso, D. J.; Cooper, S. L. *Macromolecules* **1983**, *16*, 1871.
- Galambos, A. F.; Stockton, W. B.; Koberstein, J. T.; Sen, A.; Weiss, R. A.; Russell, T. P. *Macromolecules* **1987**, *20*, 3091.
- Register, R. A.; Sen, A.; Weiss, R. A.; Cooper, S. L. *Macromolecules* **1989**, *22*, 2224.
- Weiss, R. A.; Fitzgerald, J. J.; Kim, D. *Macromolecules* **1991**, *24*, 1071.
- Fan, X. D.; Bazuin, C. G. *Macromolecules* **1993**, *26*, 2508.
- Kim, J.-S.; Roberts, S. B.; Eisenberg, A.; Moore, R. B. *Macromolecules* **1993**, *26*, 5256.
- Cimmino, S.; Di Pace, E.; Martuscelli, E.; Silvestre, C. *Polymer* **1991**, *32*, 1080.
- Gomez, M. A.; Tonelli, A. E. *Macromolecules* **1991**, *24*, 3533.
- Vittoria, V. *Polym. Commun.* **1990**, *31*, 263.
- Guerra, G.; Musto, P.; Karasz, F. E.; MacKnight, W. J. *Makromol. Chem.* **1990**, *191*, 2111.
- Reynolds, N. M.; Stidham, H. D.; Hsu, S. L. *Macromolecules* **1991**, *24*, 3662.
- Guerra, G.; Vitagliano, V.; De Rosa, C.; Petraccone, V.; Corradini, P. *Macromolecules* **1990**, *23*, 1539.
- De Rosa, C.; Rapacciuolo, M.; Guerra, G.; Petraccone, V.; Corradini, P. *Polymer* **1992**, *33*, 1423.
- Orlor, E. B.; Yontz, D. J.; Moore, R. B. *Macromolecules* **1993**, *26*, 5157.
- Orlor, E. B.; Moore, R. B. *Polym. Prepr. (Am. Chem. Soc., Div. Polym. Chem.)* **1993**, *34*(1), 852.
- Avrami, M. J. *J. Chem. Phys.* **1939**, *7*, 1103.
- Stein, R. S.; Rhodes, M. B. *J. Appl. Phys.* **1960**, *31*, 1873.
- Stein, R. S.; Misra, J. *J. Polym. Sci., Polym. Phys. Ed.* **1980**, *18*, 327.
- Lu, X.; Steckle, W. P.; Weiss, R. A. *Macromolecules* **1993**, *26*, 5876.
- Orlor, E. B.; Moore, R. B. *Polym. Prepr. (Am. Chem. Soc., Div. Polym. Chem.)* **1994**, *35*(1), 423.
- Hara, M.; Jar, P.; Sauer, J. A. *Polymer* **1991**, *32*, 1622.
- Hird, B.; Eisenberg, A. *Macromolecules* **1992**, *25*, 6466.
- Hara, M.; Eisenberg, A.; Storey, R. F.; Kennedy, J. P. In *Coulombic Interactions in Macromolecular Systems*; Eisenberg, A., Bailey, F. E., Eds.; ACS Symposium Series 302; American Chemical Society: Washington, DC, 1986; Chapter 14.
- Hay, J. N. *J. Polym. Sci., Part A* **1965**, *3*, 433.
- Wunderlich, B. *Macromolecular Physics*; Academic Press: New York, 1976; Vol. 2.
- Flory, P. J. *Principles of Polymer Chemistry*; Cornell University Press: Ithaca, NY, 1953.
- Pasztor, A. J., Jr.; Landes, B. G.; Karjala, P. J. *Thermochim. Acta* **1991**, *177*, 187.
- Gianotti, G.; Valvassori, A. *Polymer* **1990**, *31*, 473.
- Arnauts, J.; Berghmans, H. *Polym. Commun.* **1990**, *31*, 343.
- Gvozdic, N. V.; Meier, D. J. *Polym. Commun.* **1991**, *32*, 493.
- Su, Z.; Li, X.; Hsu, S. L. *Macromolecules* **1994**, *27*, 287.
- Moore, R. B.; Gauthier, M.; Williams, C. E.; Eisenberg, A. *Macromolecules* **1992**, *25*, 5769.
- Williams, C. E.; Russell, T. P.; Jerome, R.; Horron, J. *Macromolecules* **1986**, *19*, 2877.
- Roche, E. J.; Stein, R. S.; MacKnight, W. J. *J. Polym. Sci., Polym. Phys. Ed.* **1980**, *18*, 1035.
- Moore, R. B.; Bittencourt, D.; Gauthier, M.; Williams, C. E.; Eisenberg, A. *Macromolecules* **1991**, *24*, 1376.
- Eisenberg, A.; Hird, B.; Moore, R. B. *Macromolecules* **1990**, *23*, 4098.
- Mandelkern, L.; Roberts, D. E.; Halpin, J. C.; Price, F. P. *J. Am. Chem. Soc.* **1960**, *82*, 46.
- Gent, A. N. *J. Polym. Sci.* **1955**, *18*, 321.
- Napolitano, R.; Pirozzi, B. *Macromolecules* **1993**, *26*, 7225.